Local Presentation of L1 and N-Cadherin in Multicomponent, Microscale Patterns Differentially Direct Neuron Function *In Vitro*

Peng Shi, Keyue Shen, Lance C. Kam

Department of Biomedical Engineering, Columbia University, New York, New York 10027

Received 17 February 2007; accepted 8 June 2007

ABSTRACT: **The ability to pattern multiple bioactive cues on a surface is valuable for understanding how neurons interact with their complex extracellular environment. In this report, we introduce a set of methods for creating such surfaces, with the goals of understanding how developing neurons integrate multiple biologically relevant signals and as a tool for studying interactions between multiple neurons. Multiple microcontact printing steps are combined on a single surface to produce an array of polylysine nodes, interconnected by lines of proteins based on the extracellular domains of L1 or N-cadherin. Surprisingly, the N-cadherin protein could also be directly printed onto surfaces while retaining its biological activity. Rat hippocampal neurons selectively attached to the polylysine nodes, differentially extending axonal and dendritic processes along the patterns of L1 and N-cadherin, thus demonstrating control over neuron attachment and outgrowth. Combining these three biomolecules on a single surface revealed a highly complex pattern of protein recognition. Dendrites extended exclusively on N-cadherin patterns, while axons exhibited a very high degree of selectivity on L1 patterns, preferentially at distances greater than 55 μm from the cell body. At shorter distances, axonal processes recognized both L1 and N-cadherin, revealing a new aspect of neuron polarity and axon specification. This onset of L1 selectivity correlated with the establishment of intracellular L1 polarity, suggesting a functional outcome of the process of neuron polarization that has implications in development of neural tissues and creation of *in vitro* neuron networks.** Develop Neurobiol 67: 1765–1776, 2007

Keywords: **microscale; micropatterning; outgrowth; L1; N-cadherin**

INTRODUCTION

Proper development and function of neural tissues relie on the ability of neurons to navigate and interpret a complex extracellular environment; changes in the location, density, and order in which key proteins are encountered provide important cues for guiding neurons over long distances and with fine precision. Toward a better understanding of how these spatial factors influence cell growth and development, this report introduces a new system for presenting complex patterns of multiple cues to neurons *in vitro*. This system offers micrometer scale control over the layout of multiple protein patterns with few restrictions on geometry. Selectivity of hippocampal neurons to the cell–cell communication proteins L1 and N-cadherin is examined using this model, revealing a spatial/developmental modulation in how these signals are integrated by neurons.

The use of modern microfabrication techniques to direct neuron function was first introduced by Kleinfeld et al. (1988). These surfaces contained patterns of adhesive molecules against a nonpermissive background (amino- and alkyl-silanes, respectively) that restricted attachment of cells to specific areas on the substrate. Subsequent refinements and evolutions of

Correspondence to: L.C. Kam (lk2141@columbia.edu).

Contract grant sponsor: National Institutes of Health; contract grant number: NS050302.

Contract grant sponsors: Whitaker Foundation and Gatsby Charitable Foundation, UK.

Published online 20 July 2007 in Wiley InterScience (www.interscience.wiley.com).
DOI 10.1002/dneu.20553

this technique, including the use of alternative lithography strategies, microcontact printing, and chemistries for working with adhesive biomolecules, brought surface micropatterning into use in numerous fields of research. In the context of dispersed neuron culture, careful design of the adhesive pattern has allowed specification of where neuron attach, extend processes and growth cones, and a degree of control over neuron polarity (Corey et al., 1991; Fromherz et al., 1991; Stenger et al., 1998; Branch et al., 2000; James et al., 2000; Kam et al., 2001; Cornish et al., 2002). However, the permissive/nonpermissive surface approach does not capture the biomolecular complexity of environment cells encountered during development. By comparison, models such as the "stripe assay" and more recent implementations using microfabricated channels (Vielmetter et al., 1990; Esch et al., 1999; Dertinger et al., 2002; Kolpak et al., 2005) allow neurons to interact and choose between different bioactive proteins and gradients of proteins, but offer limited pattern precision and freedom of geometry.

A key study by Oliva et al. (2003) bridged these methods by combining patterns of the adhesive polypeptide poly-L-lysine (PLL) with a second set of features based on the extracellular domain of L1, a member of the immunoglobulin superfamily of cell adhesion molecules that is central to axon and neuron development. In that study, neurons selectively adhered to the patterns of PLL, while extending axons along the patterns of L1. In this report, we expand on the Oliva et al. study by adding, as a counterpoint to PLL and L1, patterns of N-Cadherin, a homophilic cell–cell communication protein that promotes both axon and dendrite outgrowth *in vitro* (Benson and Tanaka, 1998; Esch et al., 2000). This protein is thus chosen to direct dendritic outgrowth using a biologically relevant signal rather than simply a permissive surface like PLL. Patterning these three proteins together on a surface also affords opportunities to examine selectivity between these proteins in the establishment of neuron polarity and process development.

These three-component surfaces are produced by microcontact printing (Kumar et al., 1994; Singhvi et al., 1994), a technique used extensively to pattern biomolecules. In this method, an elastomer stamp containing a topological representation of a desired pattern is coated with the biomolecule of interest, and then placed in direct contact with a substrate, transferring the pattern to the substrate in the regions of contact. However, a key step in the basic microcontact printing process involves drying a solution on the stamp to reduce the presence of liquid drops, which can interfere with patterning. To avoid drying L1 on the stamp surface, which denatures the protein, Oliva et al. (2003) introduced an indirect approach in which Protein A, which is relatively resistant to deactivation by drying, is first patterned onto a surface by microcontact printing and then used to capture proteins comprised of the extracellular domain of L1 appended with Fc domain (L1-Fc molecules) from solution. In this report, we adopt this technique for patterning N-cadherin (using a variant termed Ncad-Fc), and also present the somewhat surprising result that, through modification of the basic microcontact printing technique, Ncad-Fc can be directly patterned while retaining biological activity.

METHODS AND MATERIALS

Protein Preparation

Polylysine (70–150 kDa MW; Sigma), Protein A (Pierce), and L1-Fc fusion protein (R&D Systems) were stored and prepared for use following the supplier's recommendations. Ncad-Fc was produced using a vector that encodes the extracellular domain of N-Cadherin appended with the Fc region of Human IgG and a poly-His tag. Briefly, a sequence encoding the extracellular domain of N-cadherin (generously provided by Vincenzo Cirulli, University of California San Diego) was inserted into a pcDNA3.1a-based vector encoding a GPI-tethered E-cadherin/Fc molecule (Perez et al., 2005) using standard molecular biology techniques, replacing the extracellular E-cadherin domain in that vector. The C-terminal GPI attachment sequence was then replaced with one encoding a six-residue poly-His tag and subsequent stop codon. The resultant vector was transfected into HEK-293 cells using Lipofectamine 2000 (Invitrogen), which were then grown in Dulbecco's modified Eagle's medium (DMEM) supplemented with 10% FBS and antibiotics, and selected using 400 μg/mL G418 sulfate. For protein production, cells were grown in serum-free CD293 media (Invitrogen) supplemented with 200 μg/mL G418, 4 m*M* L-glutamine, and antibiotics for 2–3 days. Ncad-Fc protein was purified from this media (supplemented with imidazole to a concentration of 50 m*M*) using an Ni-NTA agarose (Qiagen 30210) column. Purified protein was eluted with 150 m*M* imidazole in phosphate buffer, pH 8.0, concentrated by ultrafiltration (100 kDa MWCO Centricon, Millipore), and then dialyzed against PBS ph 7.4. SDS-PAGE/Coomassie and Western Blot (clone N-19, Santa Cruz Biotechnology) analyses carried out under denaturing conditions revealed a pair of bands of $\sim$100–120 kDa, appropriate for the Ncad-Fc protein.

Polylysine and Protein A were labeled with mono-reactive Cy5-NHS ester (15:1 dye to protein molar ratio, Amersham) in PBS for 1 h at room temperature. L1-Fc protein for epitope tag capture was labeled with Alexa Fluor 488

amine-reactive probe (Invitrogen) by incubating 500 μg/mL protein with dye at 1:6 molar ratio in PBS for 1 h at room temperature. Excess dye was removed by dialysis against PBS overnight at 4°C. Labeled proteins were then mixed 1:4 with unlabeled proteins for use in patterning surface for cell culture experiments.

Substrate Preparation

Round glass coverslips (15-mm German Glass, Bellco Biotech) were cleaned in Linbro 7× detergent (ICN, mixed 1:3 with deionized water) at 80°C for 30 min, rinsed extensively with deionized water, and baked at 450°C for 6 h. These substrates were modified with polylysine, L1-Fc, and Ncad-Fc, in specific combinations, following the methods described below in the order presented. For microcontact printing, polydimethylsiloxane (PDMS; Sylgard 184, Dow Corning) elastomer stamps were cast from topological masters that were prepared using standard photolithography techniques. Registration of multiple patterns was accomplished using a custom built, six-axis stage with a patterned wafer underlying the coverslip to provide an alignment reference. The transparent nature of PDMS allowed visualization of a working surface through the stamps. This apparatus currently offers practical alignment accuracy on the order of 5–10 μm, limited primarily by the elastic nature of PDMS and difficulties in preparing stamps with highly parallel surfaces.

Polylysine Coating and Patterning. Coverslips were coated with 100 μg/mL PLL in sodium borate buffer (0.1 *M*, pH 8.5) for 2 h at room temperature, washed in borate buffer, rinsed with deionized water, and blow-dried with a nitrogen gas stream. To prepare patterned polylysine surfaces, an elastomer stamp was placed in direct contact with a PLL-coated coverslip, and then processed in an air-plasma cleaner (Harrick Scientific, Ossining, NY) for 2 min; this step ablates polylysine from the regions not protected by contact with the elastomer, and yielded high-quality PLL features.

Capture-Based Patterning of L1-Fc and Ncad-Fc. PDMS stamps were treated in an air-plasma cleaner for 10 s (rendering them hydrophilic), and then coated with 10 μg/mL Protein A in deionized water for 5 min. The stamp was dried under a stream of nitrogen gas, aligned with existing patterns on a working substrate, and then placed in contact with the substrate for 10 s. After separation from the stamp, the substrate was then washed with PBS to remove extra Protein A. Substrates were then exposed to either L1-Fc (2.5 μg/mL) or Ncad-Fc (5 μg/mL) in PBS + 4% bovine serum albumin (BSA) for 1 h at 37°C, and finally rinsed in PBS.

Direct Patterning of Ncad-Fc. As an alternative method to Protein A capture, Ncad-Fc was directly patterned onto substrates by microcontact printing to create triple component surfaces. PDMS stamps (which were not treated in air-plasma and were thus hydrophobic) were coated with Ncad-Fc (20 μg/mL) in PBS 7.4 for 30 min, dried under a nitrogen stream, aligned with a working surface, and then placed in contact with the surface for 10 s. Substrates were then rinsed with PBS. To minimize degradation of Ncad-Fc activity, direct patterning of this protein was done after the PLL or Protein A patterning steps and before capture of L1-Fc. A final rinse with PBS was followed to remove excess proteins.

Protein Quantification. The surface concentration of proteins, either stamped or captured onto substrates, was estimated by microscopy-based imaging. Ncad-Fc and L1-Fc were labeled with Texas Red (succinimidyl ester, Invitrogen) before patterning; the specific dye/protein ratio was targeted to be roughly 4:1 and measured by comparing absorbance at 280 and 595 nm. A set of fluorescence standards consisted of supported lipid bilayers (Sackmann, 1996) of egg PC supplemented with specific concentrations (0.03–0.14 mol %) of Texas Red-DHPE (Invitrogen). As the structure and number of lipids per area in a membrane of specific composition are relatively well defined ($\sim 3.3 \times 10^6$ lipids/μm^2 in a bilayer of egg PC), these preparations provide a controllable and highly uniform set of calibration standards with fluorophore, fluorescence intensity, and geometry similar to that of the patterned proteins. In our implementation, the intensity of patterned proteins and calibration standards were normalized to that of fluorescence calibration beads (InSpeck beads, Invitrogen), imaged in each session under identical collection and microscopy conditions as the proteins and lipids, providing a convenient reference. Additional experiments were carried out to ensure that imaging of the bilayer, beads, and proteins resulted in a linear relation between fluorophore concentration and measured signal.

Before use in dispersed culture experiments, all substrates were sterilized by immersion in a 20-μg/mL gentamycin solution overnight, and then washed twice with sterilized PBS.

Neuron Culture and Analysis

Hippocampal cultures were prepared following the method previously described (Banker, 1991). Briefly, neurons were prepared by enzymatic and mechanical dissociation of hippocampi from E18 Sprague-Dawley rats. Cells were plated at a density of 2000–5000 cells/cm^2 on the prepared substrates in DMEM containing 10% FBS. After 2–3 h, allowing for cell attachment, the coverslips were transferred to dishes containing neurobasal medium supplemented with B27, 0.5-m*M* L-glutamate, 20-unit/mL penicillin, and 20-μg/mL streptomycin.

At specific time points (1, 4, and 14 days), cells were fixed for 15 min in 4% paraformaldehyde in PBS + 4% sucrose, permeabilized in 0.25% Triton X-100 for 10 min, and then blocked with 4% BSA in PBS for either 1 h at 37°C or overnight at 4°C. Coverslips were incubated with

primary antibodies in 4% BSA in PBS for 1 h at room temperature as indicated in the text and figures: anti-L1 (1:100, R&D Systems), anti-L1 (C-terminal, clone C20, 1:50, Santa Cruz Biotech), anti-MAP2 (1:200, Sigma), anti-N-cadherin (1:50, Santa Cruz Biotech), anti-N-cadherin (cytosolic domain, clone 13A9, 1:200, Millipore), anti-tau-1 (1:200, Chemicon), and neuronal specific anti-β-tubulin (1:2000, Covance). Substrates were then rinsed with PBS, incubated with secondary antibodies (1:500 in PBS, and labeled with either Alexa 488, Alexa 568, or Alexa 647, Molecular Probes) for 30 min, rinsed with PBS and then mounted for imaging.

Samples were imaged and recorded using a Hamamatsu C9100-02 CCD camera attached to an Olympus IX71 microscope equipped with fluorescence imaging capabilities. The MetaMorph (Molecular Devices) image analysis software was used to measure the length of processes. Data of total length and length of longest process were analyzed using ANOVA and Kruskal–Wallis procedures; significance was reported for a given value of α only when both procedures indicated a statistical difference. Data for neuron attachment and outgrowth on triple component surfaces were collected for multiple neurons (as stated in the text) over two separate samples.

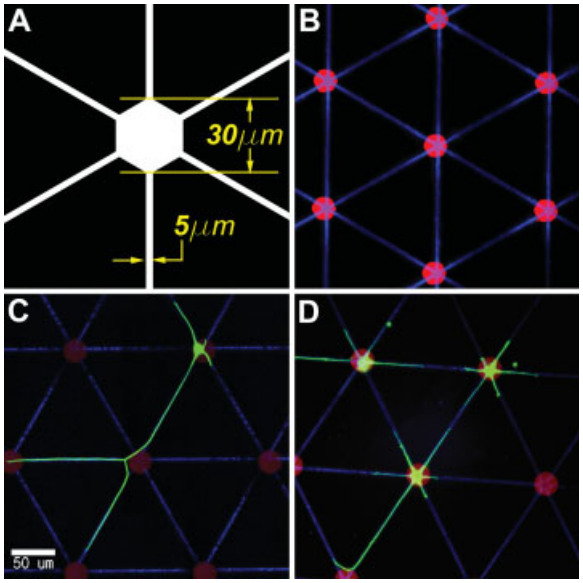

Figure 1 Directed attachment and outgrowth on two-component surfaces. (A) Schematic of the node and line pattern. (B) Surface patterned with nodes of PLL (red, Alexa 568) connected by hexagonal grids of Protein A (blue, Cy5). (C, D) One-day outgrowth of rat hippocampal neurons on surfaces pattered (C) L1-Fc and (D) Ncad-Fc. Neurons were immunostained for β-tubulin (green). Scale bar = 50 μm.

RESULTS

Neuron Outgrowth on PLL/L1-Fc and PLL/Ncad-Fc Surfaces

The basic pattern used in this report consists of a hexagonal array of 30-μm wide, hexagonal nodes spaced at 150 μm intervals and interconnected by a hexagonal lattice of 5-μm wide lines, as illustrated in Figure 1(A). This node-and-line motif, implemented as an adhesive chemistry against a nonpermissive background, has been used extensively for patterning neurons (Corey et al., 1991; Stenger et al., 1998; James et al., 2000, 2004; Vogt et al., 2004; Withers et al., 2006). Neuron somata and processes are directed to the nodes and lines, respectively, when the lines are of sufficiently small dimension. However, lines that are 5-μm wide and 150-μm long are not expected to be highly effective in directing attachment and outgrowth of hippocampal neurons (Corey et al., 1991; Withers et al., 2006). The pattern shown in Figure 1(A) is thus expected to guide process outgrowth but does not provide a high degree of control over where the cell body is localized; a key goal of this report to gain control over neuron functions by aligning patterns of different molecules, rather than through geometry.

Aligned microcontact printing was used to define lines of either L1-Fc or Ncad-Fc that interconnect the nodes of PLL. The background to these patterns is glass, which by itself is nonadhesive to neurons. An example of these surfaces is illustrated in Figure 1(B) and contains nodes of PLL (red) interconnected with lines of Protein A (blue), to which L1-Fc or Ncad-Fc were subsequently captured (Oliva et al., 2003). The surface concentration of captured proteins was measured by fluorescence microscopy, using a series of supported lipid bilayers containing defined amounts of fluorophore as concentration standard. On the basis of this method, our implementation of Protein A capture yields surface densities of $\sim$100 molecules/μm^2; similar densities of L1-Fc and Ncad-Fc were captured on these surfaces. The resultant patterns were stable with minimal loss of protein for at least 14 days, the longest examined in this report, as determined by immunofluorescence staining throughout the experiments.

These two-component surfaces were effective in directing neuron functions. By 24 h after seeding (one DIV), 82% of all cells observed on the PLL/L1-Fc surfaces were attached to the nodes (n = 98 cells over three experiments). The remaining cells had adhered to the L1-modified lines, and no cell bodies were observed on the regions of plain glass. Attach-

ment was selective on PLL/Ncad-Fc surfaces, with 62% ($n = 86$ cells) of cell bodies on the nodes at one DIV, but less preferential than on the PLL/L1-Fc surfaces. In comparison, Corey et al. (1991) found that on surfaces containing polylysine lines that measured 5-μm wide, 120-μm long, and connect nodes that are 20 μm in diameter, less than 40% of adherent cell of rat hippocampal neurons were localized to the nodes. L1-Fc and Ncad-Fc were also effective at directing and promoting early outgrowth of processes. At one DIV, neurons on PLL/L1-Fc surfaces had extended a long, often branching process, the putative axon, along the L1-Fc lines and occasionally a few short, minor neurites [Fig. 1(C)]. Neurons on PLL/Ncad-Fc surfaces [Fig. 1(D)] also elaborated a long primary process, but exhibited more extensive outgrowth of minor neurites. By one DIV, immunostaining with a tau-1 antibody was localized to the long primary processes, with further restriction to the distal end of the process at later time points, indicating axonal differentiation on all surfaces (data not shown). Axon outgrowth is compared quantitatively in Figure 2, which includes the length of the longest process and total length of all processes elaborated by neurons that attached to the PLL nodes. Data from neurons seeded onto PLL-coated coverslips, which are representative of the composition of the nodes alone, are included for comparison. At one DIV, outgrowth by neurons on L1-Fc surfaces was significantly enhanced compared with the other surfaces by both measures ($\alpha = 0.01$ for both measures). Outgrowth on Ncad-Fc lines was also enhanced compared with PLL-coated surfaces ($\alpha = 0.05$ and 0.01 for data of longest length and total length of all processes, respectively).

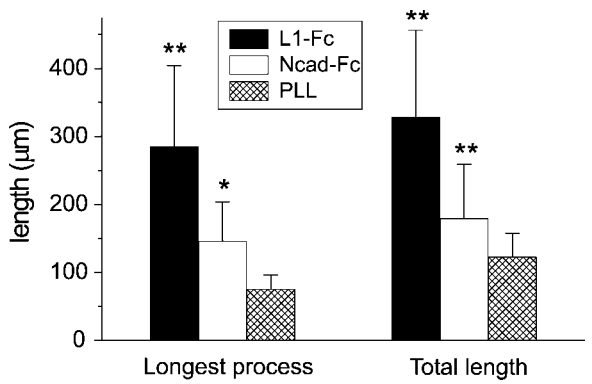

Figure 2 L1-Fc and Ncad-Fc both enhance outgrowth. By the two measures of longest process length and total length of all processes, outgrowth was enhanced on L1-Fc compared with NCad-Fc and PLL; $\alpha = 0.01$. Outgrowth on Ncad-Fc was greater than on PLL; *$\alpha = 0.05$, **$\alpha = 0.01$, compared with PLL.

Together with the observation that neurons on PLL/Ncad-Fc elaborated more and longer neurites than those on PLL/L1-Fc [Fig. 1(C,D)], these results indicate that L1-Fc is a stronger promoter of axon outgrowth, while Ncad-Fc promotes outgrowth of both axons and dendrites. Additional experiments in which the Protein A patterns were not incubated with either L1-Fc or Ncad-Fc indicated that Protein A alone does not allow outgrowth or attachment of neurons (data not shown). Furthermore, high-magnification images show that processes on the L1-Fc and Ncad-Fc lines did not exhibit a preference for the pattern edge, indicating that process outgrowth is not a result of contact guidance or other edge effect.

The differential effects of L1-Fc and Ncad-Fc are more prominent with longer time in culture. Figure 3 illustrates outgrowth at 96 h (four DIV) and 14 DIV. Signals associated with the protein patterns are omitted from these images for clarity, but are evident from the patterns of outgrowth. At four DIV [Fig. 3(A–D)], cell somata remained localized to the PLL nodes, despite overlapping between processes from adjacent cells and opportunities for cell–cell interactions. Outgrowth on all surfaces was extensive [Fig. 3(A,C)]. Given the lengths of these processes, it was difficult to assign each one to a single cell with a high degree of certainty. However, it was possible to make distinctions between axonal and dendritic processes elaborated by each cell based on staining for MAP2. On PLL/L1-Fc surfaces [Fig. 3(A)], MAP2 was predominantly localized to cell bodies and the few, short minor processes; the long primary processes were devoid of MAP2 staining and tapering morphology of dendrites [Fig. 3(B)], supportive of these structures being future axons. In contrast, neurons on the PLL/Ncad-Fc surfaces [Fig. 3(C)] elaborated multiple, tapering processes that were positive for MAP2 [Fig. 3(D)]. Cells typically had a single long process that did not stain for MAP2, indicating that these cells elaborated both axons and dendrites.

Further differences in outgrowth were observed by 14 days of culture, as shown in Figure 3(E–H). Long processes elaborated by neurons on PLL/L1-Fc patterns remained on the micropatterned lines. In contrast, processes on PLL/Ncad-Fc patterns were observed of the patterns, extending onto the regions of plain glass. MAP2 staining revealed that neurons on PLL/Ncad-Fc surfaces elaborated substantial tapering dendrites, which were primarily, but not completely, associated with the Ncad-Fc lines. On both PLL/L1-Fc and PLL/Ncad-Fc surfaces, short, thin, MAP2 positive processes could be observed near the cell bodies extending onto the plain glass regions, presumably attaching to specific, adhesive

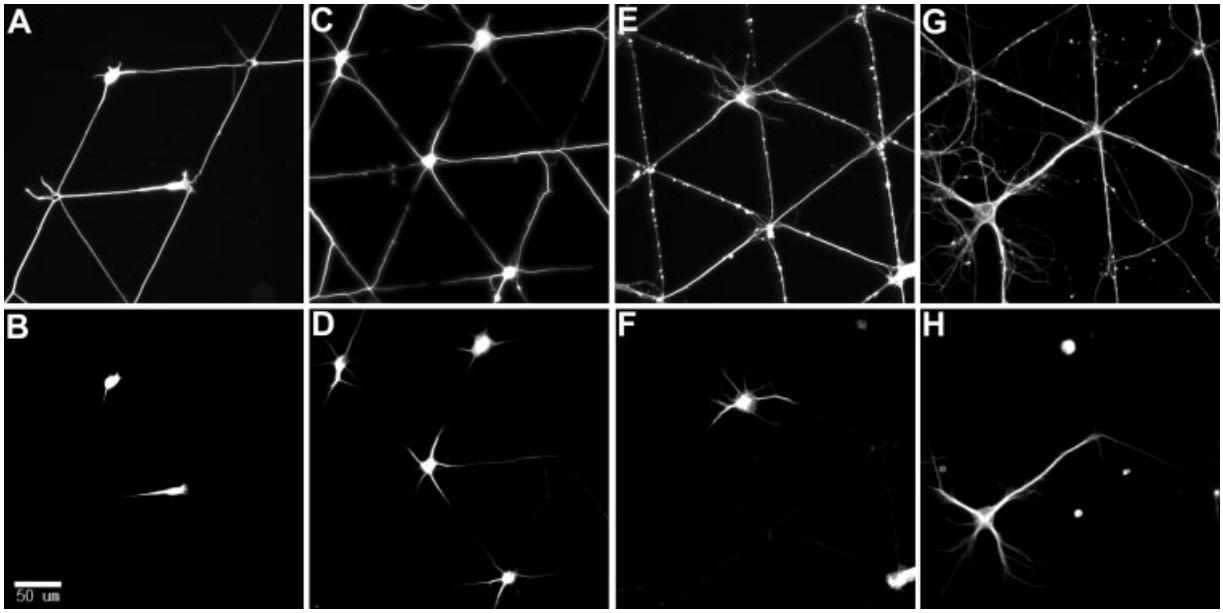

Figure 3 L1-Fc and Ncad-Fc differentially promote outgrowth on patterned surfaces. Neurons were fixed at four DIV (A–D) and 14 DIV (E–H), then stained for β-tubulin (A, C, E, G) and MAP2 (B, D, F, H). Surfaces were patterned with nodes of PLL and lines of either L1-Fc (A, B, E, F) or Ncad-Fc (C, D, G, H). The protein patterns are omitted from these images for clarity, but are evident from the process outgrowth.

proteins adsorbed from media or secreted by cells. These results suggest that L1-Fc provides better guidance of process outgrowth than Ncad-Fc. Given the differences between MAP2 staining on these surfaces, it is possible that the off-pattern processes observed on the PLL/Ncad-Fc patterns are dendrites. Alternatively, it is possible that axons as well as dendrites exhibit less selectivity for Ncad-Fc compared with L1-Fc.

These results demonstrate that micropatterned L1-Fc strongly and selectively promotes and directs outgrowth of axonal processes, while Ncad-Fc promotes outgrowth of both dendritic and axonal processes; these results are in keeping with earlier reports from the Banker group (Esch et al., 2000; Oliva et al., 2003), but further demonstrate that Ncad-Fc can be effectively patterned using the Protein A capture approach. Moreover, aligning the PLL nodes with the L1-Fc or Ncad-Fc lines offers a new degree of control over neuron attachment and outgrowth, based on protein identity rather than pattern geometry alone. It is noted that neither L1-Fc nor Ncad-Fc completely abolished cell soma attachment to the lines. It is likely that improved selectivity of this process can be achieved by reducing the width of the lines, in effect, combining biomolecular and geometric control over neuron function. However, this report aims to focus on the biomolecular cues, and will thus use exclusively lines of 5-μm width.

Direct Printing of Ncad-Fc

While many biological proteins lose their activities upon drying, we found that Ncad-Fc could be directly patterned onto substrates by modifying the microcontact printing process. Specifically, the use of a hydrophobic (rather than hydrophilic) PDMS stamp allowed the direct patterning of Ncad-Fc onto a surface while retaining bioactivity. Examples of these surfaces are shown in Figure 4, which are discussed in detail in the next section. Neuron outgrowth on PLL/Ncad-Fc surfaces produced by direct printing of Ncad-Fc was morphologically indistinguishable from that on surfaces using Protein A capture. In addition, outgrowth was similar between neurons on Protein A-captured and directly stamped Ncad-Fc at four DIV; as measured by longest process length, outgrowth on the captured and stamped Ncad-Fc lines was not significantly different (341 ± 107 μm vs. 297 ± 124 μm, respectively, data are mean $\pm$ s.d. for 25 and 17 neurons, $\alpha = 0.05$). Total length of all processes elaborated by neurons on the captured and stamped Ncad-Fc

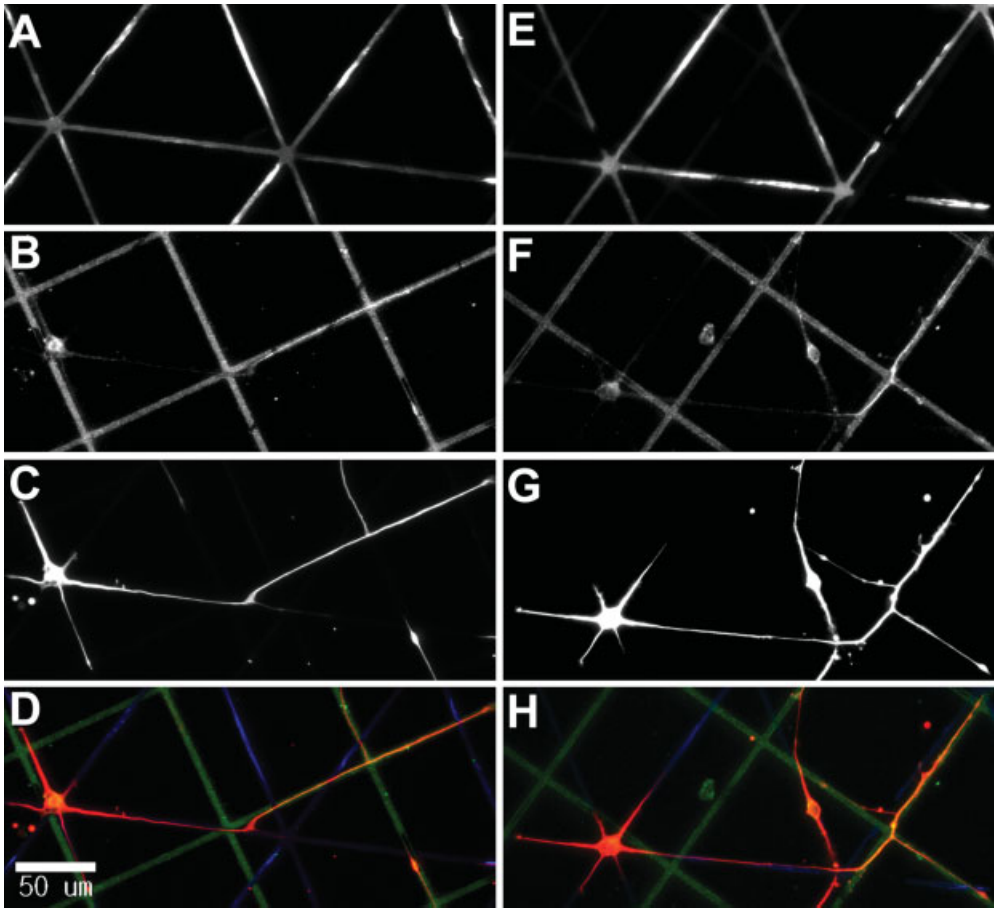

Figure 4 Neurons respond to both L1-Fc and Ncad-Fc on three-component surfaces. Two examples of 1-day outgrowth of neurons on surfaces patterned with hexagonal grids of Ncad-Fc (A, E), square grids of L1-Fc (B, F), and nodes of PLL (located at the intersections of the hexagonal grids, and omitted from these images for clarity). Neurons were stained for β-tubulin (C, G). In the merged images (D, H), Ncad-Fc, L1-Fc, and β-tubulin are shown in blue, green, and red, respectively. Neurons exhibited a typical polarized morphology, predominantly with a single primary process and several short minor processes. All of the minor processes extended along lines of Ncad-Fc, crossing lines of L1-Fc that intersected with the pattern. Putative axons often elaborate their initial segments along Ncad pattern, but turn onto L1-Fc pattern after a critical distance of 55 μm. When L1-Fc lines are encountered by these processes at distances less than 55 μm from the cell body, the major process often ignored the L1-Fc pattern, turning at the first (occasionally second) intersection with an L1-Fc feature (H). Scale bar = 50 μm.

lines was also similar (559 $\pm$ 163 μm vs. 536 $\pm$ 183 μm respectively, $\alpha = 0.05$). As measured by fluorescence microscopy (and using the supported lipid bilayer standards), direct patterning of NCad-Fc resulted in a surface concentration of 1000 molecules/μm^2, which varied by 20% between features stamped onto a substrate. This represents an almost 10-fold increase in surface concentration compared with Protein A-based capture, which might offset any loss in protein activity that results from drying the protein solution. The ability to directly stamp Ncad-Fc on a surface provided a straightforward mechanism for producing three-component surfaces, as described in the next section.

Neuron Outgrowth on PLL/L1-Fc/ Ncad-Fc Surfaces

Three-component surfaces were produced by combining PLL ablation, microcontact printing of Protein A (with later capture of L1-Fc), and direct patterning of Ncad-Fc on the same substrate. These substrates

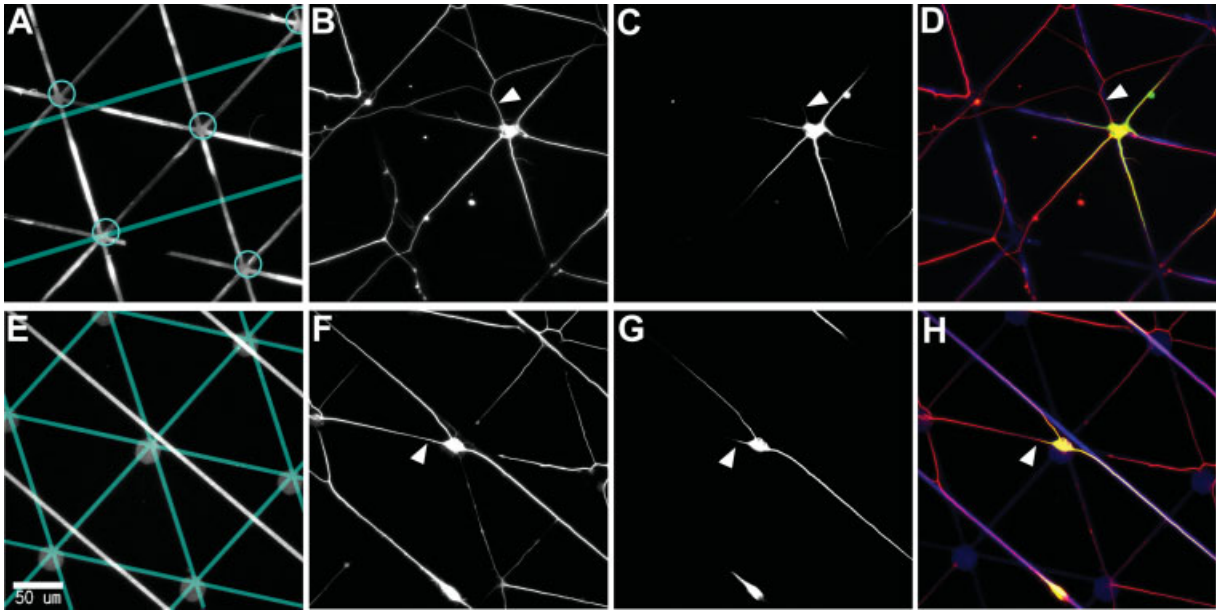

Figure 5 Combined patterns of L1-Fc and Ncad-Fc provides selective control over axonal and dendritic outgrowth. Representative images illustrating 4-day outgrowth on three-component surfaces patterned with hexagonal grids of (A–D) Ncad-Fc and (E–H) L1-Fc. Panels A and E show surface-patterned proteins, indicated as follows: Ncad-Fc grids, grey lines; L1-Fc, blue lines (identified in a long-exposure image as Ncad-Fc and L1-Fc were labeled with the same fluorophore); PLL, circles (either drawn in or shown in grey) at the intersection of the hexagonal grids. Panels B and F: β-tubulin staining for neurons. Panels C and G: MAP2 staining for dendrites. Panels D and H: merged images. Arrowheads indicate axonal processes. Scale bar = 50 μm.

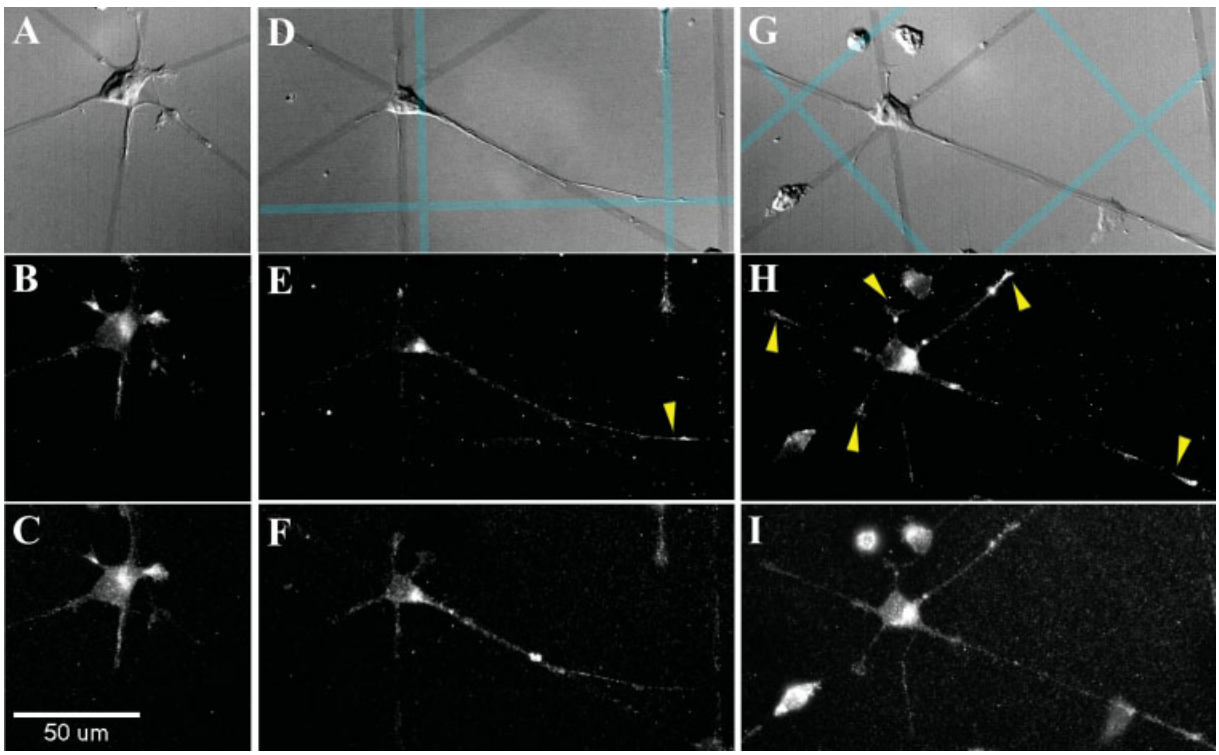

Figure 6

provided a spatially rich environment in which neurons encountered multiple protein cues under a variety of configurations. Figure 4 shows two examples of 1-day attachment and outgrowth of neurons on surfaces patterned with PLL nodes, a hexagonal grid of Ncad-Fc connecting these nodes [Fig. 4(A,E)], and a square grid pattern of L1-Fc lines measuring 5 μm in width and spaced 100 μm apart [Fig. 4(B,F)]. For visualization purposes, unlabeled and Cy5-labeled Ncad-Fc proteins were mixed before use, while patterns of L1-Fc and neurons were detected by immunostaining. Merged images of these patterns and neuron outgrowth are shown in Figure 4(D,H).

At one DIV, neuron cell somata attached predominantly to the PLL nodes or patterns of Ncad-Fc, consistent with the selectivity observed on the PLL/Ncad-Fc surfaces; the following discussion is limited to neurons for which the cell body was attached to a PLL node. These neurons exhibited a typical polarized morphology, with predominantly a single primary process and several short minor processes. All minor processes extended along lines of Ncad-Fc, crossing lines of L1-Fc that intersected with the pattern.

Outgrowth of the axonal process by each cell was more complicated. This section begins by focusing on neurons that attached to PLL nodes that were coincident with both lines of L1-Fc as well as lines of Ncad-Fc. The longest process elaborated by these neurons showed little selectivity between the L1-Fc and Ncad-Fc lines at one DIV [Fig. 4(A–D)]. That is, the segment of these processes closest to the neuron cell body extended along lines of Ncad-Fc roughly twice as often as on L1-Fc (of 18 cells that fit this criteria, 12 elaborated their longest process on Ncad-Fc), close to the overall 3:1 ratio of Ncad-Fc to L1-Fc lines presented at that intersection. If this proximal segment was on a line of L1-Fc, the process remained on patterns of L1-Fc, sometimes turning onto intersecting patterns of L1-Fc, but rarely turning onto patterns of Ncad-Fc.

Now focusing on neurons for which the proximal segment of the longest process had extended on a pattern of Ncad-Fc, this axonal process eventually turned onto a line of L1-Fc at some distance further from the cell body. However, the point at which this process turned was dependent on distance from the cell body to this line of L1-Fc. Specifically, if the first intersection of the Ncad-Fc pattern and a line of L1-Fc was greater than 55 μm from the center of the PLL node, the process preferentially turned onto this line in 76% of such observations ($n = 21$ neurons). By the second intersection between an Ncad-Fc pattern and L1-Fc line, over 90% ($n = 51$ cells) of the processes had turned onto the L1-Fc. In contrast, if a line of L1-Fc intersected the Ncad-Fc pattern at a distance closer than 55 μm, the longest process often remained on the Ncad-Fc pattern (47%, $n = 31$); Figure 4(E–H) illustrates a neuron that does not respond to two lines of L1-Fc, both of which are within 45 μm of the PLL node. Together, these observations demonstrate a distance- or outgrowth-dependent selectivity for process extension along L1-Fc rather than Ncad-Fc. That is, selectivity for L1-Fc increases with increasing neurite length. Our somewhat artificial cutoff of 55 μm represents a characteristic length for this effect; while selectivity for L1-Fc over Ncad-Fc is seen for individual processes at both longer and shorter distances, 55 μm provides a useful descriptor of the population behavior.

For all geometries, once the longest process extended onto a line of L1-Fc, it remained on that line, although, as reported elsewhere (Esch et al., 2000; Oliva et al., 2003), processes were frequently observed to deviate off the pattern at sharp corners, which we also interpret as likely the result of tension being generated in these processes after the growth cone followed the corner. This longest process often branched or turned at intersections of L1 lines, but rarely returned to patterns of Ncad-Fc (less than 3% of our 57 observations). Lastly, when the longest process from a cell on an Ncad-Fc line intersected with one of L1-Fc, it was presented with a choice of multiple angles at which to extend. In our observations, 85% ($n = 39$ observations) of these intersections, the process bent at an angle less than 90° (the direction that introduced less bend) rather than selecting a sharper turning radius. As previously suggested

Figure 6 Selectivity for L1-Fc correlates with polarization of endogenous L1. Representative images of Stage 2 (A–C) and Stage 3 (D–F, G–I) neurons. Panels A, D, and G show a DIC image overlaid with patterns of Ncad-Fc (hexagonal, grey lines) and L1-Fc (square grid, light blue), identified from long-exposure fluorescence images. Panels B, E, and H illustrate neuron-endogenous L1, as detected using an antibody specific for the cytosolic domain of L1. Panels C, F, and I illustrate neuron-endogenous N-cadherin, detected using a cytosolic domain-specific antibody. Yellow arrows in E and H indicated concentrations of L1 at the ends of processes elaborated by these axons. Scale bar = 50 μm.

(Withers et al., 2006), this preference may reflect the endogenous stiffness of microtubules, which greatly restricts bending and reduces the likelihood of microtubule growth at angles greater than 90°.

By four DIV, neurons exhibited extensive outgrowth that prevented complete assignment of processes to a specific neuron. This outgrowth is illustrated by the two examples in Figure 5. Both images illustrate neurons on patterns of PLL nodes. Figure 5(A–D) illustrates a pattern of nodes interconnected by a hexagonal lattice of Ncad-Fc, with a series of parallel lines of L1-Fc overlaid on these surfaces. Immunofluorescence staining for MAP2, together with process morphology, confirms that axons on these surfaces exhibit a strong selectivity for the L1-Fc patterns, whereas dendrites are found on the Ncad-Fc patterns. Changing the ratio of Ncad-Fc and L1-Fc lines, by inversing two protein patterns as shown in Figure 5(E–H), which illustrates an array of PLL nodes interconnected by hexagonal lattice of L1-Fc superimposed by parallel lines of Ncad-Fc, resulted in fewer dendrites that were still associated with the Ncad-Fc lines. Together, these results demonstrate that neurons can concurrently respond to both L1-Fc and Ncad-Fc with a high degree of specificity.

To better understand the outgrowth-dependent selectivity of axonal processes for L1-Fc illustrated in Figure 4, neurons were stained for endogenous L1 and Ncad (the cellular ligands for the Fc fusion proteins), using antibodies generated against the cytosolic domains of these proteins. Neurons were fixed at 6 or 12 h after seeding to capture neurons that are morphologically Stage 2 or Stage 3 (Craig et al., 1994); this process occurs at earlier time points for rat hippocampal neurons on L1 or Ncad than on the standard polylysine surface. As illustrated in Figure 6(A–C), Stage 2 neurons exhibited a nonpolarized distribution of L1, in which this protein is present in each process as well as in the cell body. In contrast, most Stage 3 neurons exhibited a polarized distribution of L1, in which this protein is localized to the cell body and single (occasionally two), long process, the axon [Fig. 6(D–F)]. Importantly, neurons for which the axon initially extended on Ncad-Fc but turned onto L1-Fc exhibited this polarization of L1. However, an additional population of neurons was observed, which were morphologically Stage 3 with, but L1 was not localized to a single, axonal process but also present in minor neurites, as illustrated in Figure 6(G–I). It is in these neurons that the longest process, if extended initially on a line of Ncad-Fc, did not respond to lines of L1-Fc. In contrast to endogenous L1, N-cadherin was observed in the cell body and processes, with no preferential distribution in relation to the axonal process [Fig. 6(C,F,I)]. These patterns of expression, including the observation that morphological polarization precedes L1 segregation, agrees with earlier reports and current understanding of neuron polarization (van den Pol and Kim, 1993; Craig et al., 1994; Benson and Tanaka, 1998).

DISCUSSION

By aligning and combining multiple patterning steps on a single surface, and taking advantage of the surprising observation that Ncad-Fc can retain significant biological activity through a microcontact printing process, we introduce the use of multicomponent surfaces to examine how neurons integrate cues in the highly complex extracellular environment. While the factors that allow Ncad-Fc, but not L1-Fc, to retain activity when directly stamped are not known, it is anticipated that other cell–cell communication proteins will show activity when patterned using this modified process.

In themselves, the separate observations of axon and dendrite outgrowth on surfaces containing nodes of PLL and lines of captured L1-Fc or Ncad-Fc are in keeping with previous studies of there proteins (Esch et al., 1999, 2000; Oliva et al., 2003), and not surprising. However, combining L1-Fc and Ncad-Fc lines with PLL nodes on the same surface provided an opportunity to compare neuron interaction with these cell–cell communication proteins, and revealed a complex pattern of cell response. In particular, while both L1 and N-cadherin promote axon outgrowth, our results demonstrate that under our surface patterning conditions axons preferentially respond to L1-Fc, turning onto lines of this protein and not responding to patterns of Ncad-Fc. Immunostaining of fixed cells suggests that at intersections between lines of these proteins, axons will turn along L1-Fc lines that provide a smaller angle of turn, supporting earlier studies that correlate the geometry of growth cone response to the mechanical properties of cytoskeletal elements (Burden-Gulley and Lemmon, 1996; Suter and Forscher, 1998; Withers et al., 2006). Live cell imaging suggests that at intersections of L1-Fc and Ncad-Fc lines, growth cones attempt to interact concurrently with both proteins as it extends beyond this junction, eventually collapsing onto L1-Fc as the lines of proteins diverge beyond the reach of the growth cone (data not shown); continued interaction with the Ncad-Fc line may provide an additional factor that promotes shallow turning angles by the growth cone. Measurements of surface concentration of L1-Fc and Ncad-Fc suggest that this selectivity is not simply a

matter of surface concentration; indeed, the areal concentration of Ncad-Fc is ~ 10 times higher than that of L1-Fc on the three component surfaces. Moreover, our observation of distance- or outgrowth-dependent selectivity for L1-Fc over Ncad-Fc suggests that a more complex interplay of factors is involved in L1 response.

Specifically, our data suggest that polarization of L1 occurs before neurons respond strongly to L1. This is somewhat surprising, as L1 is initially expressed in all compartments of neurons at initial development stages, becoming later polarized to the newly specified axon; in other words, L1 is present in the neurite that is or will become the axon both before and after polarization. Continued axon growth over days is associated with increased localization of L1 to the axon (van den Pol and Kim, 1993). While it is possible that this increased L1 concentration on the axon cell surface may in itself explain the distance- or outgrowth-dependent selectivity for L1-Fc we observed, the relatively fast onset of this selectivity suggests that additional aspects of establishment of neuron polarity are involved. This process is manifested morphologically by the transition of a neuron from Stage 2 to Stage 3, in which one of the competing processes breaks symmetry and begins prolonged extension establishing itself as the eventual axon, and molecularly by the compartmentalization of proteins to the axonal or dendritic/cell body compartment. Our results suggest that polarization of L1, measured as the presence of this protein in all processes as opposed to the axon alone, happens after the morphological transition to Stage 3 [Fig. 6(G–I)]. A previous report (Sampo et al., 2003) suggests that polarization of L1, like NgCAM, is effected by targeted delivery of this protein to the axonal compartment; our observed delay in L1 polarization may thus reflect the slow removal of L1 from the nonaxonal compartment. Building on this, we speculate on two possible mechanisms behind the observed delay in L1 selectivity. First, strong L1-based neurite outgrowth in established neurons requires endocytosis and recycling of this protein in the growth cone (Kamiguchi and Yoshihara, 2001), which involves additional proteins that exhibit axon polarization such as CRMP-2 (Inagaki et al., 2001; Nishimura et al., 2003). Delayed outgrowth selectivity for L1 may thus reflect the need for polarization of not only L1, but also these other proteins, which may be on a similar timescale. Second, the signaling and cycling complexes for L1 may be present in all neurites in the prepolarized state, but inhibited by factors being transported from neighboring processes, a common motif in neuron polarity. As process specification progresses (in this case, following the timescale of L1), these inhibitory signals decrease, turning on the strong response to L1. In both scenarios (and, indeed, others) the presence of L1 in the nonaxonal processes allows neurite outgrowth along patterns of L1, without generating a strong, polarizing response itself; this last aspect would explain why neurons can extend neurites onto L1, but these are not preferentially designated to become axons. This complex pattern of L1 selectivity may shed light onto new aspects of tissue development. In effect, this phenomenon represents insensitivity to neighboring neurons, promoting interactions or migration to more distant structures.

These results also have large implications in the *in vitro* creation of directed neuron networks. Patterning of surfaces with permissive/nonpermissive chemistries has been a powerful tool for directing the interactions of neurons with each other and with engineered surfaces, such as substrate-embedded electrodes (Ravenscroft et al., 1998; James et al., 2000, 2004; Vogt et al., 2005). However, the lack of appropriately arranged biomolecular cues may be associated with a loss of functionality of these systems; Vogt et al. (2004) determined that synapse formation between neurons on micropatterned surfaces was similar to that on unpatterned surfaces, once corrected for the space restriction of the pattern. In our attempt to capture this complexity, our initial approach was to include patterns of L1-Fc that intersect the PLL node to direct axon outgrowth between neurons in such networks; clearly, our observation that the proximal segments of the axonal processes exhibited little selectivity for L1-Fc when given an alternative of Ncad-Fc suggest that this approach would not be effective. However, placing tracks of L1-Fc a distance from the cell body, in conjunction with controlling the angles of the various intersections, would be effective in redirecting axonal processes and provide the level of control needed to form defined networks of neurons *in vitro*. In combination with geometric control over neuron function, as well as other approaches to modifying surfaces, we anticipate that these surfaces will find widespread use in basic studies of single- and multiple-neuron function.

REFERENCES

Banker G. 1991. Culturing Nerve Cells. Cambridge, MA: MIT Press.

Benson DL, Tanaka H. 1998. N-Cadherin redistribution during synaptogenesis in hippocampal neurons. J Neurosci 18:6892–6904.

Branch DW, Wheeler BC, Brewer GJ, Leckband DE. 2000. Long-term maintenance of patterns of hippocampal pyramidal cells on substrates of polyethylene glycol and microstamped polylysine. IEEE Trans Biomed Eng 47:290–300.

Burden-Gulley SM, Lemmon V. 1996. L1, N-cadherin, and laminin induce distinct distribution patterns of cytoskeletal elements in growth cones. Cell Motil Cytoskeleton 35:1–23.

Corey JM, Wheeler BC, Brewer GJ. 1991. Compliance of hippocampal neurons to patterned substrate networks. J Neurosci Res 30:300–307.

Cornish T, Branch DW, Wheeler BC, Campanelli JT. 2002. Microcontact printing: A versatile technique for the study of synaptogenic molecules. Mol Cell Neurosci 20:140–153.

Craig AM, Banker G, Craig AM, Banker G. 1994. Neuronal polarity. Ann Rev Neurosci 17:267–310.

Dertinger SKW, Jiang X, Li Z, Murthy VN, Whitesides GM. 2002. Gradients of substrate-bound laminin orient axonal specification of neurons. Proc Natl Acad Sci USA 99:12542–12547.

Esch T, Lemmon V, Banker G. 1999. Local presentation of substrate molecules directs axon specification by cultured hippocampal neurons. J Neurosci 19:6417–6426.

Esch T, Lemmon V, Banker G. 2000. Differential effects of NgCAM and N-cadherin on the development of axons and dendrites by cultured hippocampal neurons. J Neurocytol 29:215–223.

Fromherz P, Schaden H, Vetter T. 1991. Guided outgrowth of leech neurons in culture. Neurosci Lett 129:77–80.

Inagaki N, Chihara K, Arimura N, Menager C, Kawano Y, Matsuo N, Nishimura T, et al. 2001. CRMP-2 induces axons in cultured hippocampal neurons. Nat Neurosci 4:781–782.

James CD, Davis R, Meyer M, Turner A, Turner S, Withers G, Kam L, et al. 2000. Aligned microcontact printing of micrometer-scale poly-L-lysine structures for controlled growth of cultured neurons on planar microelectrode arrays. IEEE Trans Biomed Eng 47:17–21.

James CD, Spence AJH, Dowell-Mesfin NM, Hussain RJ, Smith KL, Craighead HG, Isaacson MS, et al. 2004. Extracellular recordings from patterned neuronal networks using planar microelectrode arrays. IEEE Trans Biomed Eng 51:1640–1648.

Kam L, Shain W, Turner JN, Bizios R. 2001. Axonal outgrowth of hippocampal neurons on micro-scale networks of polylysine-conjugated laminin. Biomaterials 22:1049–1054.

Kamiguchi H, Yoshihara F. 2001. The role of endocytic L1 tafficking in polarized adhesion and migration of nerve growth cones. J Neruosci 21:9194–9203.

Kleinfeld D, Kahler KH, Hockberger PE. 1988. Controlled outgrowth of dissociated neurons on patterned substrates. J Neurosci 8:4098–4120.

Kolpak A, Zhang J, Bao ZZ. 2005. Sonic hedgehog has a dual effect on the growth of retinal ganglion axons depending on its concentration. J Neurosci 25:3432–3441.

Kumar A, Biebuyck HA, Whitesides GM. 1994. Patterning self-assembled monolayers: Applications in material science. Langmuir 10:1498–1511.

Nishimura T, Fukata Y, Kato K, Yamaguchi T, Matsuura Y, Kamiguchi H, Kaibuchi K. 2003. CRMP-2 regulates polarized Numb-mediated endocytosis for axon growth. Nat Cell Biol 5:819–826.

Oliva AA Jr, James CD, Kingman CE, Craighead HG, Banker GA. 2003. Patterning axonal guidance molecules using a novel strategy for microcontact printing. Neurochem Res 28:1639–1648.

Perez TD, Nelson WJ, Boxer SG, Kam L. 2005. E-Cadherin tethered to micropatterned supported lipid bilayers as a model for cell adhesion. Langmuir 21:11963–11968.

Ravenscroft MS, Bateman KE, Shaffer KM, Schessler HM, Jung DR, Schneider TW, Montgomery CB, et al. 1998. Developmental neurobiology implications from fabrication and analysis of hippocampal neuronal networks on patterned silane-modified surfaces. J Am Chem Soc 120:12169–12177.

Sackmann E. 1996. Supported membranes: Scientific and practical applications. Science 271:43–48.

Sampo B, Kaech S, Kunz S, Banker G. 2003. Two distinct mechanisms target membrane proteins to axonal surface. Neuron 37:611–624.

Singhvi R, Kumar A, Lopez GP, Stephanopoulos GN, Wang DI, Whitesides GM, Ingber DE. 1994. Engineering cell shape and function. Science 264:696–698.

Stenger DA, Hickman JJ, Bateman KE, Ravenscroft MS, Ma W, Pancrazio JJ, Shaffer K, et al. 1998. Microlithographic determination of axonal/dendritic polarity in cultured hippocampal neurons. J Neurosci Methods 82:167–173.

Suter DM, Forscher P. 1998. An emerging link between cytoskeletal dynamics and cell adhesion molecules in growth cone guidance. Curr Opin Neurobiol 8:106–116.

van den Pol AN, Kim WT. 1993. NILE/L1 and NCAM-polysialic acid expression on growing axons of isolated neurons. J Comp Neurol 332:237–257.

Vielmetter J, Stolze B, Bonhoeffer F, Stuermer CAO. 1990. In vitro assay to test differential substrate affinities of growing axons and migratory cells. Exp Brain Res V81:283.

Vogt AK, Stefani FD, Best A, Nelles G, Yasuda A, Knoll W, Offenhausser A. 2004. Impact of micropatterned surfaces on neuronal polarity. J Neurosci Methods 134:191–198.

Vogt AK, Wrobel G, Meyer W, Knoll W, Offenhausser A. 2005. Synaptic plasticity in micropatterned neuronal networks. Biomaterials 26:2549.

Withers GS, James CD, Kingman CE, Craighead HG, Banker GA. 2006. Effects of substrate geometry on growth cone behavior and axon branching. J Neurobiol 66:1183–1194.